



COMPARISON OF THE SCATTERING OF AN OPERATING AND A QUIESCENT FAN

Stefan SACK¹, Mats ÅBOM¹,
Korcan KUCUKCOSKUN², Christophe SCHRAM²

¹ *Royal Institute of Technology, The Marcus Wallenberg Laboratory,
Teknikringen 8, 100 44 Stockholm, Sweden*

² *von Karman Institute for Fluid Dynamics, Rhode-St-Gense, B-1640,
Belgium*

SUMMARY

The paper in hand compares the scattering matrix of an axial fan in operating and quiescent state obtained with sophisticated in-duct measurements and enhanced sensor positions. The results showed low differences for the transmission and reflection in both, amplitude and phase, which could be beneficial to simplify scattering computation.

INTRODUCTION

Noise from ducts and pipes in air-conditioning systems influences the cabin comfort of air-crafts essentially. Reaching low levels of sound emission is crucial to create enjoyable environments for the passengers and to decrease stress symptoms and tiredness for the crew. The Environmental Control System (ECS) is important to guarantee the required temperature and air quality, but it is a key contributor to acoustic noise within the air-craft. The complex mechanisms of noise generation in the ECS have not been sufficiently investigated. Especially the propagation of higher acoustic modes and their scattering and reflection behaviors at certain subcomponents e.g. mufflers, fans, junctions and valves is mostly unknown. However, the cut-on frequencies of higher circumferential and radial wave-modes can become distinctly perceptible by the human ear for ECS-ducts with common diameters.

Within the framework of the European project "Idealvent" the generation and scattering of higher acoustic modes emitted by the ECS will be investigated in detail. Acoustic measurements on

different ECS components are taken in order to establish analytical noise models and to validate simulation codes. The extracted data can serve as input for calculating the sound scattering of the ECS as a multi-port network which facilitates the development of feasible noise reduction strategies. As a part of this project, the paper in hand shows an N -port approach of the order $N = 8$ to describe the acoustic reflection and scattering for the first 6 circumferential and 2 radial modes within a straight duct.

The measurement approach has been presented in previous work [1, 2] and is now applied in order to characterize the scattering matrix and the source vector of an axial fan. The method is applicable either experimentally or numerically. The focus of this paper is to compare the scattering matrix of an operating fan with a none-operating test case. The quiescent state, however, is less sophisticated. A good agreement of both results can help to facilitate the measurement and the modeling. Especially numerical investigations would simplify significantly if the scattering were computed without blade-flow interaction. Also the experimental set-up would benefit from more precise measurements taken in absence of mean-flow and hence with lower background noise.

MULTI-PORT APPROACH

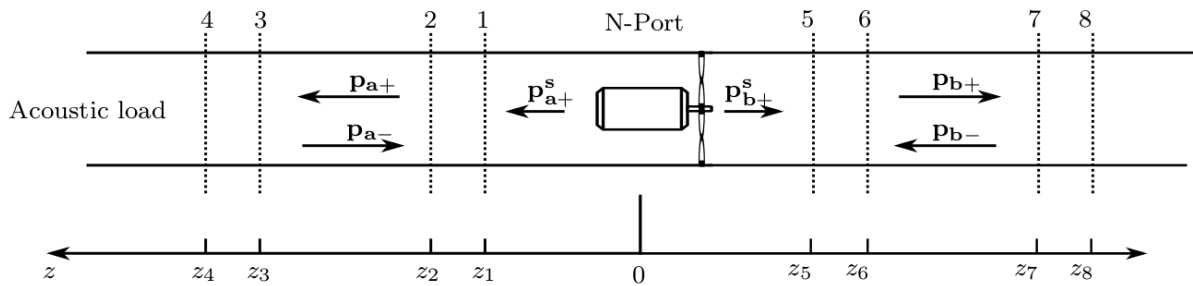


Figure 1: Sketch of a duct with acoustic load and multi-port source. The source vector contains the acoustic modes evoked by the source. The sound waves created by the acoustic load are reflected and transmitted at the multi-port. The indexes + and - denote the direction of the propagation. The dotted lines indicate the microphone sections.

An acoustic element, as shown in Figure 1, may be treated as a multi-port in such a way that it fulfills the equation

$$\underline{p}^+ = \underline{\underline{S}} \underline{p}^- + \underline{p}_s^+ , \quad (1)$$

where \underline{p}^\pm contains the incident and outgoing acoustic modes in frequency domain, $\underline{\underline{S}}$ is the scattering matrix, and \underline{p}_s^+ is the source vector [1]. Equation 1 is a linear, time-invariant system of equations. The parameters in $\underline{\underline{S}}$ and \underline{p}_s^+ can be determined in two steps, either numerically or experimentally. First, external acoustic loads are induced, e.g. with loudspeaker sources. These external loads need to be stronger than the actual multi-port source. To uncouple the N propagating modes, at least N linear independent sound fields have to be induced both up- and downstream. The measured sound fields can be decomposed in mode vectors using the analytical solution of the mode propagation within a straight duct

$$\underline{p} = \underline{\underline{M}} \underline{p}^\pm , \quad (2)$$

where $\underline{\underline{M}}$ is the transformed modal matrix, that contains eigen-shapes and eigen-values of all modes in up- and down-stream direction. The vector \underline{p} contains the sound fields as a function of

frequency for at least $2N$ spatial points at both, the inlet and the outlet section of the multi-port [1- 4].

Once the scattering matrix is computed, the source vector can be extracted from the decomposed sound field created by the multi-port itself. Reflections within the test-rig are eliminated by deploying the scattering matrix of the multi-port and the reflection matrix of the test-rig terminations. Uncorrelated noise is reduced according to Holmberg et al. [5] with cross-correlated microphone pairs. The source vector can then be computed

$$\begin{aligned} \underline{p}_1^+ &= [\underline{E} - \underline{SR}] \underline{C}_1^{-1} \underline{p}_1 \\ \underline{p}_2^+ &= [\underline{E} - \underline{SR}] \underline{C}_2^{-1} \underline{p}_2 \end{aligned} \quad (3)$$

where \underline{E} is the identity matrix, $\underline{p}_{1/2}$ are two vectors of cross-correlated microphone pairs, \underline{R} is the reflection of the rig terminations, and \underline{C}_i is a modified modal matrix

$$C_i = [\underline{M}_{i+} + \underline{M}_{i-} \underline{R}] \quad (4)$$

TEST-RIG DESIGN

The test-rig used in this paper was designed to meet the requirements which were mainly imposed by the properties of the fan. The fan characteristics are presented in table 1. According to the blade-passing-frequency (BPF), the measurement range was chosen to be 500 Hz to 3500 Hz. However, this range included a number of cut-on frequencies of higher order acoustic modes. The cut-on frequency of a certain mode (m,n), where m denotes the circumferential and n the radial mode order can be found in table 2. Since the circumferential modes always appear in pairs, a total amount of 8 modes including 2 radial and 6 circumferential modes was propagating within the frequency range under consideration.

Table 1: Characteristics of the fan in use.

Radius max	83.775 mm	Rotor blades	15
Radius outlet	86.250 mm	Stator blades	10
Radius inlet	74.700 mm	BPF	2800 HZ
BLH	186.66 Hz		

Table 2: Cut-on frequencies of the duct modes ($r=75$ mm).

Mode order	(1,0)	(1,0)	(2,0)	(0,1)	(3,0)	(4,0)
Cut-on frequency / Hz	0	1337	2217	2781	3049	3858

According to equation 1 and 2, a total number 32 sensors and 16 sound sources were required to perform the full multi-port characterization. However, it was shown that an over-determination in sources and sensors may significantly increases the measurement results [2,4]. For the paper in hand, a source over-determination of the order 8 was realized, which resulted in a total number of 24 sources equally distributed up- and downstream. As sensors, 32 B&K 4938-A11 high pressure microphones were flush-mounted to the channel walls.

In order to solve equation 1 and 2, two matrix inversions had to be performed. Those matrices however, which are defined by the sensor and source positions, become easily singular for certain frequencies. Therefore, the microphone and loudspeaker sections were optimized according to the procedures described in [1]. These previous investigations showed, that the condition number of \underline{M} and \underline{p}^- might be a sufficient measure for the quality of the chosen microphone and loudspeaker positions. Figure 2 shows the condition number of the transformed modal matrix for different source configurations. The peaks in the grey line correspond to singular frequencies evoked by mode-coupling. The applied configuration (black line) is only singular at the cut-on frequencies, which is unavoidable. However, due to the decreasing sensor and source over-determination for higher order modes, the condition number increases with the mode order, which indicates an augmenting sensitivity for measurement uncertainties.

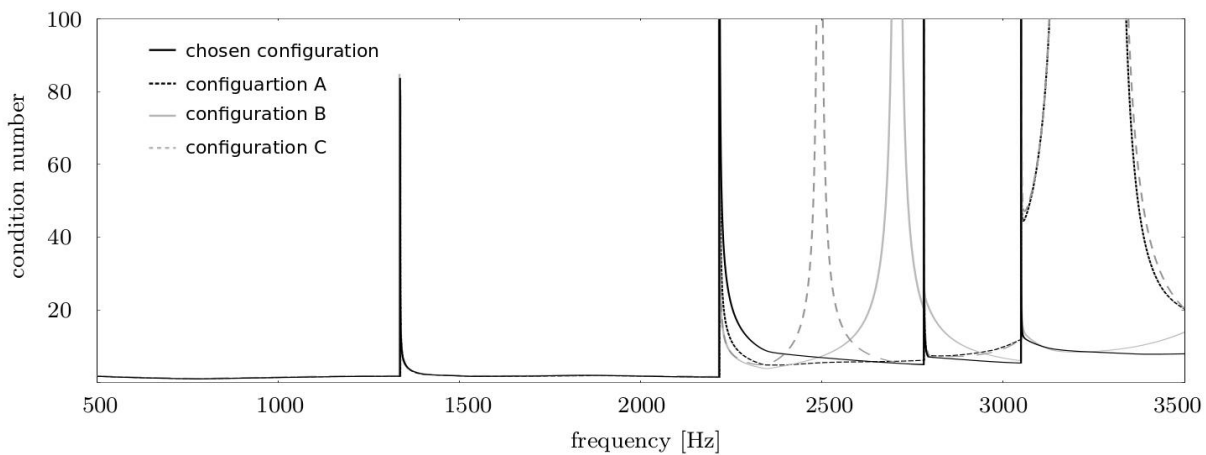


Figure 2: Condition number of \underline{M} for different sensor configuration with singularities within the measurement range.

MEASUREMENTS

Procedure

To induce the external sound fields, the loudspeaker sources were driven with step-sinusoidal signals. The total measurement time was reduced by exciting 4 loudspeakers on different frequencies at the same time. The necessary acquiring time for each frequency point was determined by the coherence between loudspeakers and microphones in previous test drives to hold the uncertainties in the microphone signals beneath 2 percent.

As a first step of measurements and as a case of validation, the scattering of an empty duct in presence of mean flow was ascertained for which the analytical solution is well known [5]. Figure 3 shows the reflection coefficients for the 8 propagating duct modes from downstream direction together with the analytical solution.

In a second step, the measurements of the fan in quiescent state and on operating state were taken. For the operating state, the measurement time was increased to achieve lower noise levels. Figure 4 and Figure 5 compare the transmission coefficients for the 8 propagating modes in amplitude and phase, respectively. The magnitude of the reflection coefficient is presented in Figure 6.

Discussion

As it can be seen in the empty duct measurements (Figure 3), the experimental set-up is suitable to capture all modes. Apart from the (3,0) mode, all modes are measured with high precision. The uncertainties at the cut-on frequencies are caused by the singularities within the matrix inversions. In the plain-wave coefficients, the strong coupling between the (0,0)-mode and (0,1)-mode is conspicuous at the cut-on of the (0,1)-mode. The small bumps in the reflection coefficients may be induced by structural vibrations within the test-rig.

The comparison of operating and quiescent fan shows good agreement. The shape of the spectra and the order of magnitude is similar for the investigated fan states for both, the reflection coefficient as well as for the transmission coefficient (Figure 4 and Figure 6). The none-operating fan shows slightly higher transmission between 1500 Hz and 2000 Hz, especially for the plane wave mode. Due to increasing flow noise, the measurements of the operating fan become noisier for higher order modes. The phase shift in Figure 5 changes with mode order and is due to the convective flow created by the rotating fan blades. The influence of the flow on the wave number could be computed after the post-processing [1] in order to correct the phase spectrum.

CONCLUSION

The determination of the scattering matrix of an axial fan may be difficult on operation frequency due to turbulent flow fields and blade-flow interactions. The paper in hand therefore compared the reflection and transmission coefficients of an operating fan with its far less sophisticated quiescent state.

The scattering matrix of an axial fan could be measured with an advanced measurement setup even for higher order modes and under presence of turbulent flow. The condition number of the modal matrices together with measurements taken on an empty duct revealed the achievable quality of the measurements.

The two investigated fan states show a good agreement in reflection and transmission coefficients. Only the phase spectrum is shifted due to the established flow field of the operating fan. It can be concluded, that mainly the fan geometry accounts for the sound scattering. Depending on the required accuracy, assemblies with such kind of fan may be therefore treated as quiescent geometries, what greatly simplifies the investigations.

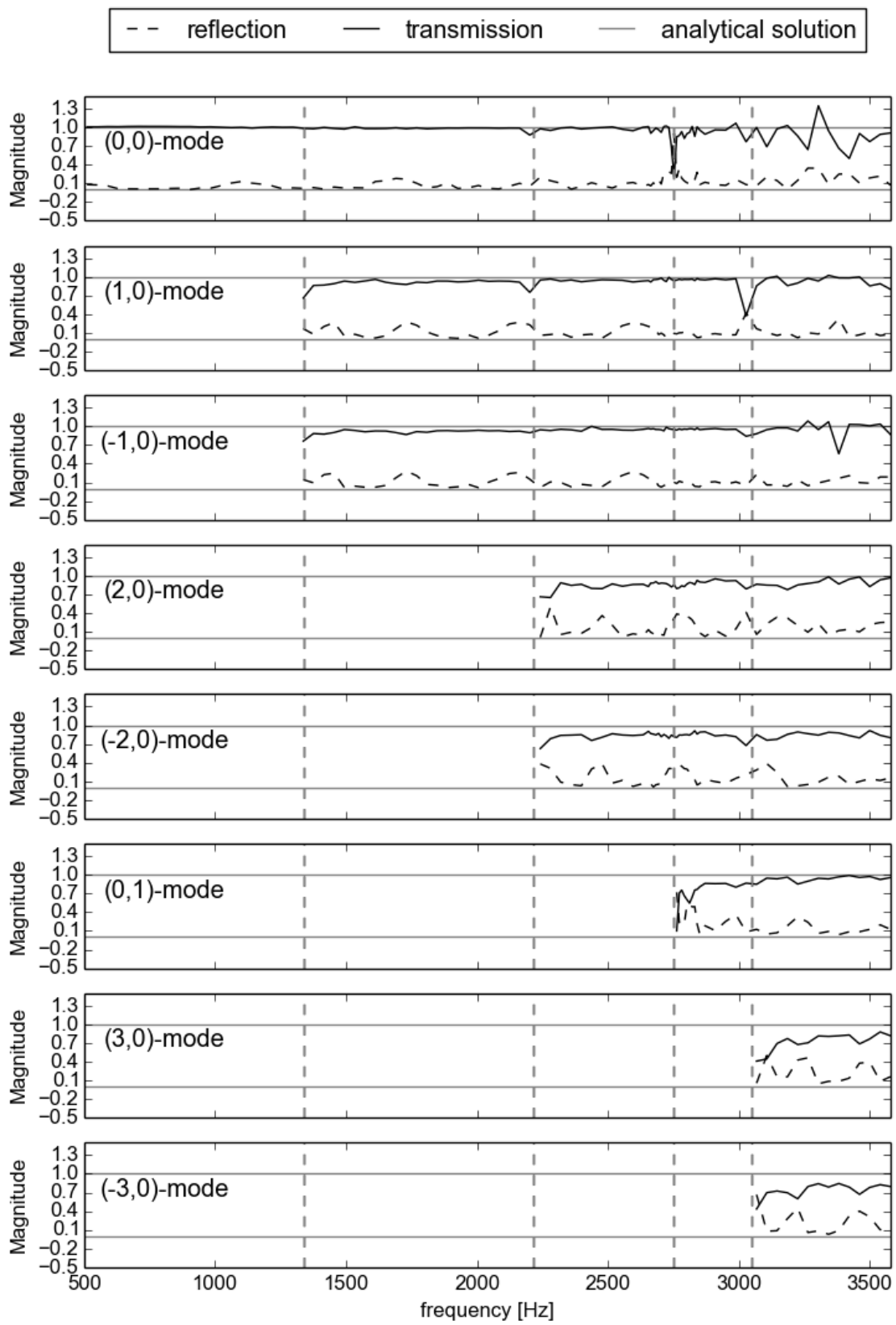


Figure 3: Empty duct with flow ($M=0.1$) to show the achievable quality of the measurement.

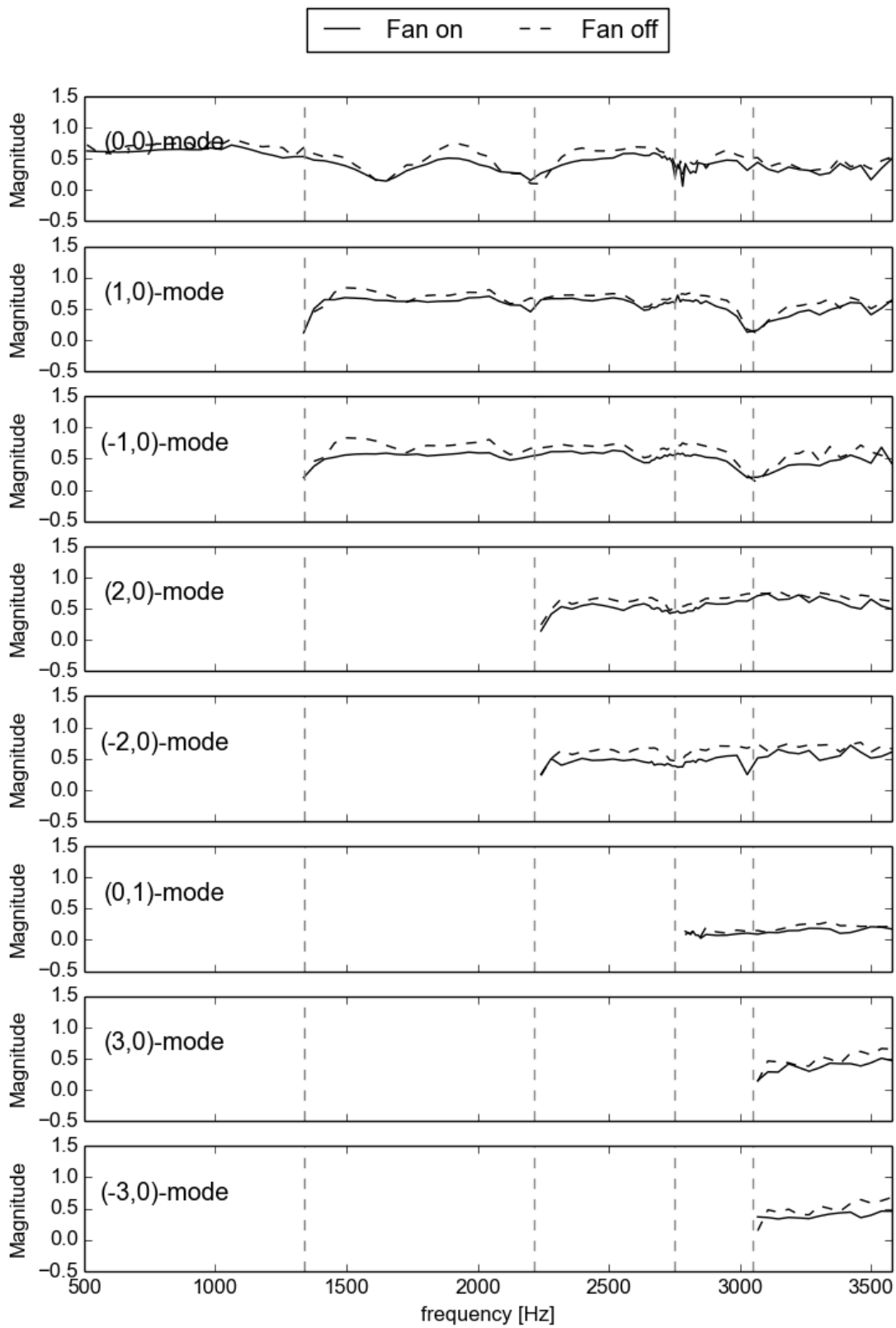


Figure 4: Magnitude of the transmission coefficient of all propagating modes for two fan states.

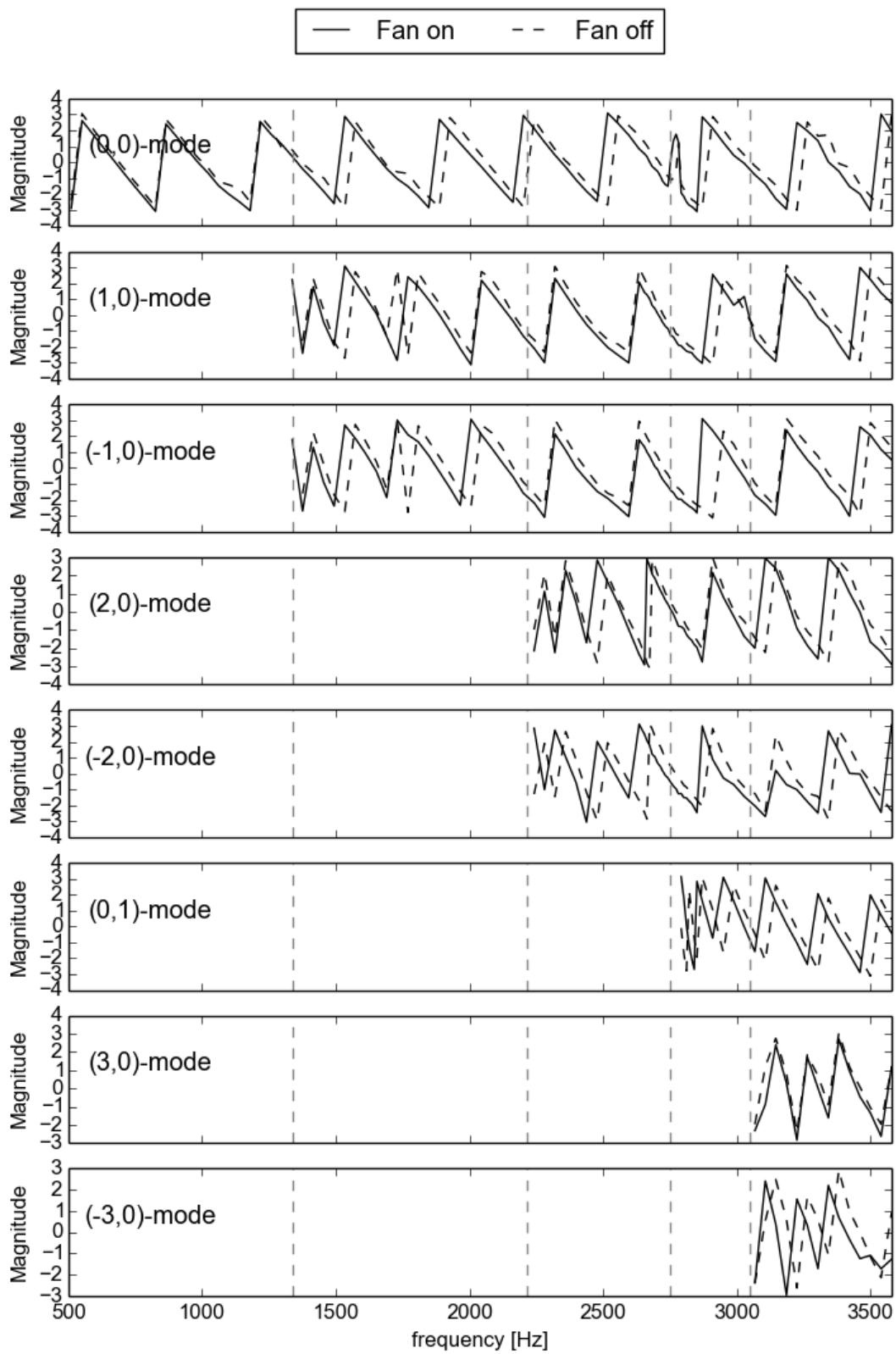


Figure 5: Phase of the transmission coefficient of all propagating modes for two fan states.

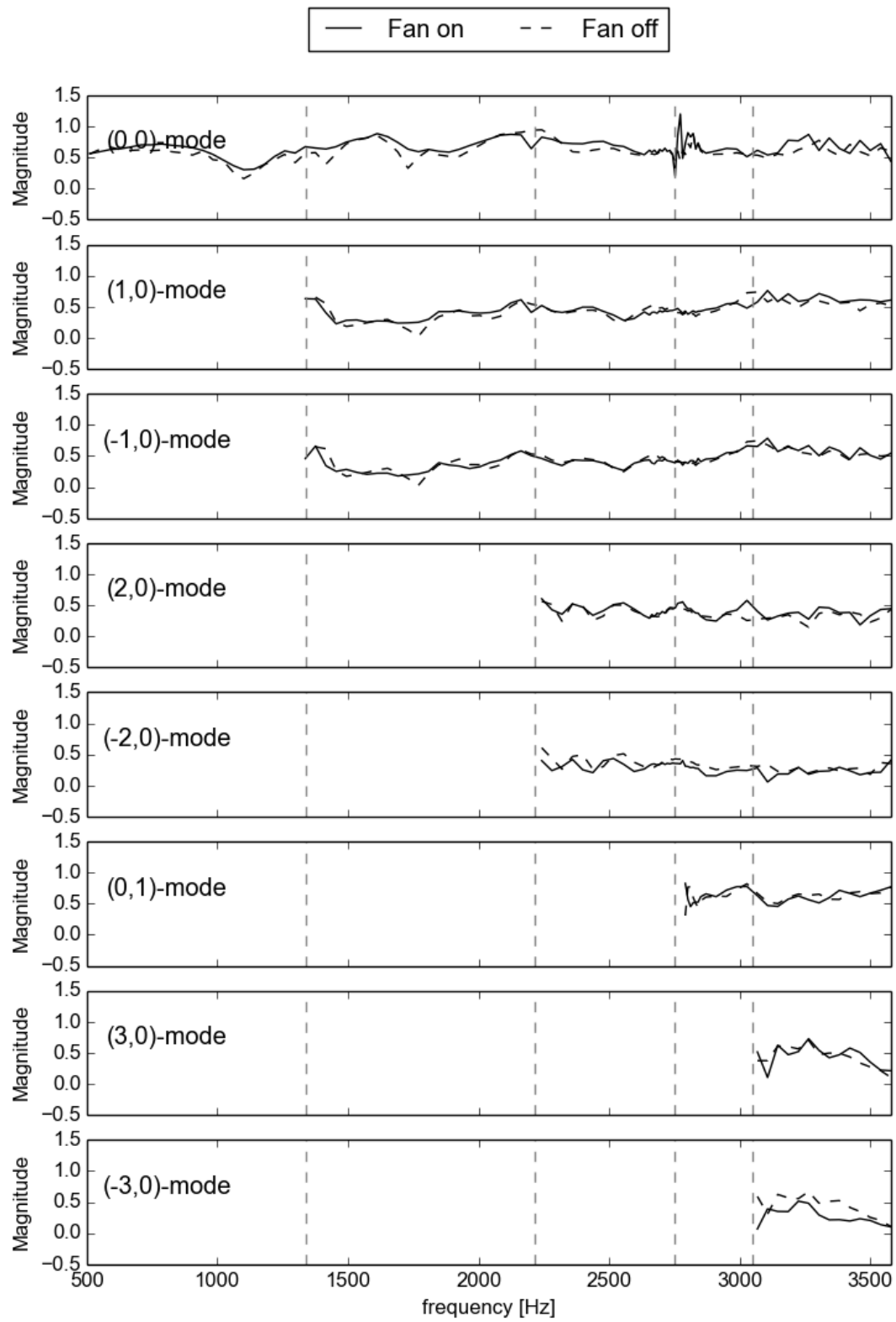


Figure 6: Magnitude of the reflection coefficient of all propagating modes for two fan states.

BIBLIOGRAPHY

- [1] J. Lavrentjev, M. Åbom - *Characterization of Fluid Machines as acoustic multi-port Sources*. Journal of Sound and Vibration, 197, **1996**
- [2] S. Sack, M. Åbom, S. Cristophe, K. Kucukcoskun - *Generation and scattering of acoustic modes in ducts with flow*, AIAA, **2014**
- [3] J. Lavrentjev, M. Åbom - *A Measurement Method for Determining the Source Data of Acoustic Two-Port Sources*, Journal of Sound and Vibration, **1995**
- [4] A. Holmberg, M. Åbom, H. Bodén - *Accurate experimental two-port analysis of flow generated sound*, Journal of Sound and Vibration, **2011**
- [5] P. Morse, K. Ingard, *Theoretical Acoustics*, Princeton University, **1986**